10. Lowry, B. A., S. A. Rice, and P. Gray, *ibid.*, **40**, 3673 (1964).
11. Mathur, G. P., and George Thodos, *AIChE J.*, **11**, 613 (1965).
12. Matschke, D. E., and George Thodos, *J. Petrol. Technol.*, **12**, 67 (1960).
13. Naghizadeh, J., and S. A. Rice, *J. Chem. Phys.*, **36**, 2710 (1962).
14. Palyvos, J. A., and H. T. Davis, *J. Phys. Chem.*, **71**, 439 (1967).
15. Ramanan, P., M. S. thesis, Univ. Kentucky, Lexington (1971).
16. Rice, S. A., and A. R. Allnatt, *J. Chem. Phys.*, **34**, 2144 (1961).
17. Robinson, R. C., and W. E. Stewart, *Ind. Eng. Chem. Fundamentals*, **7**, 90 (1968).
18. Stiel, L. I., and George Thodos, *Can. J. Chem. Eng.*, 187 (1965).
19. Winn, E. B., *Phys. Rev.*, **80**, 1024 (1950).
20. Woessner, D. E., B. S. Snowden, R. A. George, and J. C. Melrose, *Ind. Eng. Chem. Fundamentals*, **8**, 779 (1969).

Manuscript received December 11, 1970; revision received October 27, 1971; paper accepted November 2, 1971.

The Peak Pool Boiling Heat Flux from a Sphere

JAGJIT S. DED and JOHN H. LIENHARD

Mechanical Engineering Department
University of Kentucky, Lexington, Kentucky 40506

A hydrodynamic prediction is formulated for the peak nucleate boiling heat flux on spheres. It employs no empirical constants but it is justified by an experimental correlation of the vapor blanket thickness at the equator of the sphere. The prediction compares very favorably with 27 original data obtained by the transient calorimeter method in both water and N_2 on spheres of different sizes. It also compares well with the data of prior investigators for a large range of size, gravity, and boiled liquids. Assumptions as to the vapor removal configuration are supported with photographic observations of the boiling process.

The objective of this work is to provide a hydrodynamic prediction of the peak heat flux q_{max} on spheres and to support this theory with observations of both q_{max} and the dynamics of vapor removal. This study is part of an ongoing effort to predict the influence of gravity on the peak and minimum heat fluxes.

It is interesting that some of the earliest variable gravity studies [by Merte et al. (*1*, *2*)] used spherical heaters. These studies more-or-less demonstrated the one-quarter-power dependence of q_{max} on the gravity g predicted by Zuber (3) for flat-plate heaters,* that is,

$$q_{maxF} \simeq \frac{\pi}{24} \rho_g^{1/2} h_{fg} [\sigma g(\rho_f - \rho_g)]^{1/4} \qquad (1)$$

They also provided a variety of q_{max} data for nitrogen boiling on spheres of different size under a range of gravities.

Most studies of boiling from spheres have used the transient calorimeter technique. A heated sphere with a thermocouple mounted in the center has been quenched in the boiling liquid and allowed to cool. This involves making the tacit assumptions that the Biot Number $Bi = hR/k$ is small and that the process is quasi-static. Bergles and Thompson (*4*), quoting from earlier sources, suggest that Bi at q_{max} should not be much more than 0.4 for accuracy. But they also warn against the second possible source of error—namely that the boiling process might fail to accommodate rapidly enough to be quasi-static.

More recently Veres and Florschuetz (5) argued that Bergles and Thompson's accommodation discrepancy was in fact the result of a failure to use the same heaters in both the transient and steady state tests. But the heaters for the two situations differed little in shape and in surface condition. However, Veres and Florschuetz obtained results that were quite similar to steady state data when they quenched the same heaters, as long as the heaters were kept fairly clean during the quench. But sufficiently heavy oxide layers, accrued during the preheat prior to quenching, led to a deviation from steady state results. Veres and Florschuetz also provided additional q_{max} data for spheres.

Correspondence concerning this paper should be addressed to J. H. Lienhard.

* This is the appropriate form of Zuber's prediction as long as the system pressure is not near the critical pressure.

In 1964 and 1965, Bobrovich, Gogonin, and Kutateladze (6) and Lienhard and Watanabe (7) independently showed that q_{max} data for cylinders (and other configurations) could be correlated with functional equations of the form

$$\frac{q_{max}}{q_{maxF}} = f(R'); \quad R' \equiv R\sqrt{g(\rho_f - \rho_g)/\sigma} \qquad (2)$$

It was further shown in (8) that such a correlation is legitimate if: 1. The surface chemistry is comparable in all cases, but the roughness is of comparatively little importance. 2. The geometry is such as to permit a free movement of induced flows around the body (true for cylinders and spheres but not for flat plates). 3. The system pressure is not close to the critical point.

The expression, equivalent to Equation (2), for the minimum heat flux q_{min} is

$$\frac{q_{min}}{q_{minF}} = f(R') \qquad (3)$$

The hydrodynamic prediction of q_{min} on horizontal cylinders (9) took exactly this form. Subsequently Sun and Lienhard (10) developed a hydrodynamic theory for q_{max} on cylinders which took the form of Equation (2). We shall seek an analytical expression of this form for q_{max} on spheres, using methods that have much in common with those in (10). In so doing we presume some familiarity with the hydrodynamic theory of q_{max} and q_{min}.*

PREDICTION OF q_{max} FOR SPHERES

The vapor removal configuration near q_{max} depends upon the size of the sphere relative to the most susceptible Taylor-unstable wavelength λ_d for the liquid-vapor interface. This wavelength was shown by Bellman and Pennington (11) to be† the critical wavelength times $\sqrt{3}$ or

$$\lambda_d = 2\pi\sqrt{3}\sqrt{\sigma/g(\rho_f - \rho_g)} \qquad (4)$$

Zuber's original hydrodynamic theory for q_{maxF} was based on the assumption that vapor jets are spaced on a grid with mesh size λ_d. However, for spheres no interfacial waves can exist when the diameter is less than the minimum, or critical, wavelength (that is, when $2R \leq \lambda_d/\sqrt{3}$ or when $R' \leq \pi$). In this case we anticipate a vapor removal configuration such as is shown in Figure 1. Bubbles on the lower hemisphere slide up and around, merging with one another, eventually forming a single jet above the sphere. The radius of this jet R_j is comparable in magnitude to the radius of the sphere itself. The actual value of R_j and the thickness of the vapor blanket δ are quantities to be established subsequently.

When $2R > \lambda_d$, the sphere should accommodate more than one jet, but how many? One might look for jets spaced on a λ_d-mesh grid above the sphere, but photographs don't show this sort of pattern even when R' is large. Actually the vapor tends to slide up one side of the sphere and to jet up around the equator. Accordingly, we propose to treat just four jets arranged as shown in Figure 2.

In either configuration, the peak heat flux occurs when the escaping jets reach the velocity U at which they are Helmholtz unstable. At this point an energy balance gives

$$q_{max} = \rho_g h_{fg} U \frac{A_j}{4\pi R^2} \qquad (5)$$

where A_j is the combined jet area. To express A_j in terms of δ, we employ an idea recently developed by Lienhard and Dhir (14). They rationalized Sun's (10) vapor blanket thickness data, by arguing that the velocity in the blanket at the equator must match that in the jet. Since roughly half as much vapor passes the equator as flows through the jet, we have for $\delta/R << 1$

$$A_j = 2\,[2\pi(R + \delta/2)\,\delta] \qquad (6)$$

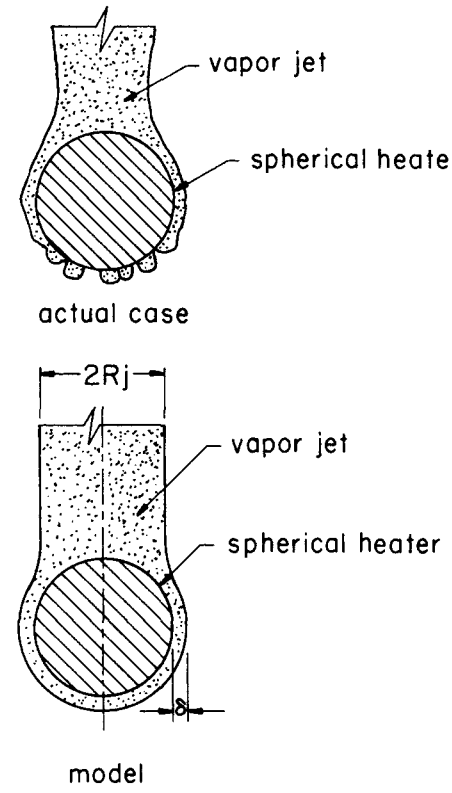

Fig. 1. Vapor removal configuration near q_{max} on a sphere for $2R \leq \lambda_d/\sqrt{3}$.

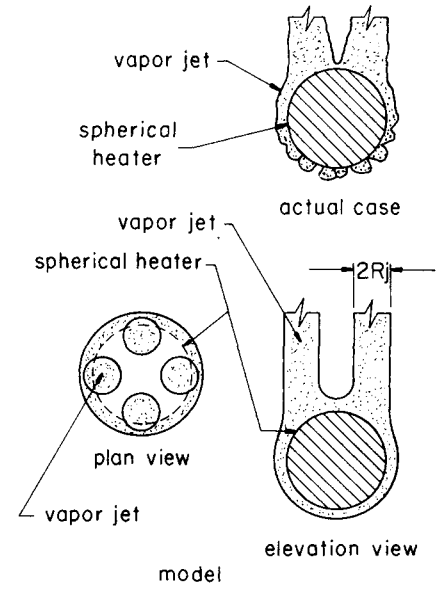

Fig. 2. Vapor removal configuration near q_{max} on a sphere for $2R > \lambda_d$.

* Following Zuber's thesis (3), these ideas were further rationalized and elaborated in a number of subsequent works, for example, (12) and (13).

† Equation (4) is a two-dimensional result. Although past work (9) has revealed influences of three-dimensional curvature around very small heaters during film boiling, it was shown in (10) that these effects are lost in the more ragged liquid-vapor interfaces near q_{max}.

so*

$$q_{max} = \rho_g h_{fg} U \frac{(R + \delta/2)\delta}{R^2} \quad (7)$$

The velocity U, as given by Lamb (*15*) for a Helmholtz unstable wave, is

$$U = \sqrt{2\pi\sigma/\rho_g \lambda_H} \quad (8)$$

where λ_H is the wavelength of the Helmholtz unstable disturbance. We have also used $\rho_g/\rho_f << 1$; and taken the velocity of the incoming liquid to be negligible. Next we must identify those disturbances of length λ_H that we expect to be triggered by U.

For the single jet on a small sphere we shall follow Zuber's and Sun's successful assumption, and take this disturbance to be the Rayleigh unstable wave in the jet. Lamb (*15*) shows that this λ_H is equal to $2\pi R_j$ or (since $R_j = \sqrt{A_j}/\pi$ or $2\sqrt{(R + \delta/2)\delta}$ $\lambda_H = 4\pi\sqrt{(R + \delta/2)\delta}$. Using this λ_H in Equation (8), and the resulting U in Equation (7), we get

$$q_{max}|_{\text{small } R} = \sqrt{\frac{\sigma\rho_g}{2}} h_{fg} \frac{[(R + \delta/2)\delta]^{3/4}}{R^2} \quad (9)$$

For the large spheres, the jets become large and the surface tension forces that shape the Rayleigh waves become very weak. However, if $2R >> \lambda_d$, the wavelength λ_d is probably picked up from the intervening interface by the departing jets. It then becomes the dominant nonuniformity in the jets so $\lambda_H = \lambda_d$. Substituting Equation (4) in Equation (8), and the resulting U in Equation (7), we obtain

$$q_{max}|_{\text{large } R} = \frac{\sqrt{\rho_g}}{3^{1/4}} h_{fg} \sqrt[4]{g\sigma(\rho_f - \rho_g)} \frac{(R + \delta/2)\delta}{R^2} \quad (10)$$

Finally, using the definitions of R' and q_{maxF} and defining a dimensionless vapor blanket thickness, $\Delta \equiv \delta\sqrt{g(\rho_f - \rho_g)/\sigma}$, we reduce Equations (9) and (10) to

$$\left.\frac{q_{max}}{q_{maxF}}\right|_{\text{small } R'} = \frac{12\sqrt{2}}{\pi} \frac{[(R' + \Delta/2)\Delta)]^{3/4}}{R'^2} \quad (11)$$

and

$$\left.\frac{q_{max}}{q_{maxF}}\right|_{\text{large } R'} = \frac{8(3)^{3/4}}{\pi} \frac{(R' + \Delta/2)\Delta}{R'^2} \quad (12)$$

The same dimensional considerations that led to Equation (2) also require that Δ must be a unique function of R'. Therefore Equation (12) is consistent with Equation (2). We shall subsequently obtain the relationship $\Delta = \Delta(R')$ from an experimental correlation.

All of the prior applications of Equation (2), for example, (*6, 7, 8,* and *10*) have borne out the experimental fact that

$$\lim_{R' \to \infty} \left[\frac{q_{max}}{q_{maxF}} \text{ or } \frac{q_{min}}{q_{minF}} \right] = \text{constant} \quad (13)$$

Reference (*8*), in fact, correlated the 14 q_{max} data then available for spheres and suggested that the constant in this configuration should be about 0.84. This will agree with Equation (12) if (for large R') $\Delta = 0.134\ R'$ or alternatively if $\delta/R = 0.134$. Equation (12) thus exhibits the correct limiting behavior as long as the vapor removal patterns for large spheres are all geometrically similar.

* If we simply assumed for small jets that $A_j = \pi R^2$, we could get (*á priori*) from Equation (6), that $\delta = 0.225R$. We shall return to this point subsequently.

EXPERIMENT

Figure 3 shows the general layout of the experiment we used to measure q_{max} and δ in both nitrogen and double-distilled water. The test heaters were 0.635, 1.27, and 2.54 cm. copper spheres with iron-constantan thermocouples mounted in the center. The water-quenched spheres were heated to about 500°C. in an oven and the nitrogen-quenched spheres were stabilized at room temperature. In both cases the spheres were then quenched in the test beaker.

For boiling in water, a 13 cm. I.D. glass beaker was placed on a hotplate which kept the water saturated. A 15 cm. I.D. double-walled, clear glass, vacuum-insulated Dewar was used to hold the liquid nitrogen. It was kept saturated by heat leakage from the atmosphere, and the double wall prevented condensation on the outside so that clear photographs could be made.

Details of the sphere mounting are shown in Figure 4. An additional thermocouple was placed near the surface of a 2.54-cm. diam. sphere for use in some of the water runs. This facilitated an experimental indication of the extent of the failure of the lumped-capacity (or uniform sphere temperature) assumption. The worst case (2.54 cm. sphere in water) yielded only about 2°C. temperature difference between the two thermocouples.

The spheres were polished with 500 grit emery cloth and the surface was cleaned carefully before each run. Since runs made with a sphere cleaned in acetone and runs made with one simply sanded and then washed in water gave identical results, both procedures were used. The acetone rinse procedure was used in obtaining most of the data with which we shall compare our results. While some light oxidation formed during the preheat, we avoided serious surface deterioration by using moderate preheat temperatures and by starting each test with a clean sphere. This procedure, in accordance with the results of Veres and Florschuetz, should give data that are equivalent to steady state results.

The data in (*4*) and (*5*) as well as the work of Berenson (*16*) showed that while q_{max} was fairly insensitive to surface

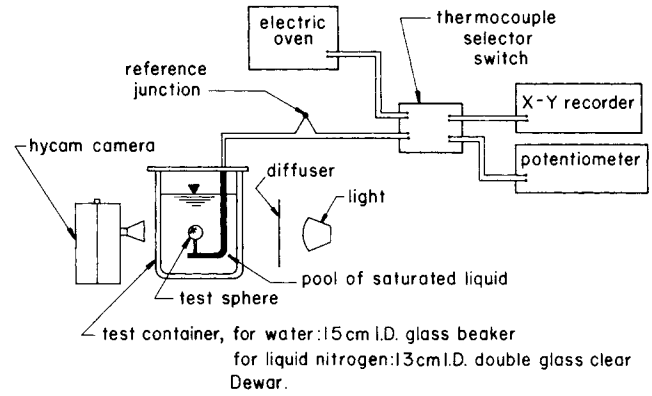

Fig. 3. Schematic diagram of the experiment.

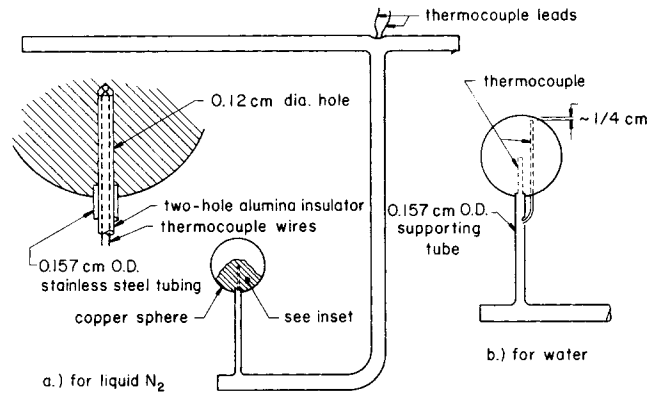

Fig. 4. Test spheres for water and liquid nitrogen.

conditions, q_{min} is seriously altered even by minor changes in surface conditions. We also calculated q_{min} data for some runs in water and found them to be generally high. We accordingly have avoided presenting any of our q_{min} data in the present study.

Additional details of the experimental apparatus and procedure are given by Ded (*17*) and will not be reproduced here.

HEAT FLUX DATA REDUCTION AND RESULTS

The basic output of an experimental run was a temperature-time history such as is shown in Figure 5. The heat flux was obtained from these curves by noting that

$$q = -\rho_h \frac{\frac{4}{3}\pi R^3}{4\pi R^2} c_p(T) \frac{dT}{dt} = -\rho_h c_p(T) \frac{R}{3} \frac{dT}{dt} \tag{14}$$

in those cases for which $Bi < 0.4$. The location of the peak heat flux point (or point of maximum negative slope) has been noted on the figure.

Figure 6 shows the results of measuring slopes from Figure 5 and using Equation (14) to compute the heat flux. In this case, however, the Biot number reached its highest value of 0.85. Accordingly, a more precise procedure than that involved in Equation (14) was required to obtain q_{max} from the raw T_{center} versus t plot. For the $Bi > 0.4$ runs we employed the following computational method:

The transient heat conduction equation for a spherically symmetrical body was solved numerically beginning with a known uniform temperature distribution at $t = 0$, and using the boundary conditions $dT/dr = 0$, and T equal to a measured function of time on $r = 0$. A simple Euler's method was used and the increments were chosen so that $\alpha\Delta t/(\Delta r)^2 = 0.139$. Rerunning the program with larger and smaller values of $\alpha\Delta t/\Delta r^2$ did not alter the results. The instantaneous temperature distribution was then averaged over the volume and T in Equation (14) was replaced with this average value.

Figure 6 includes the distributed parameter computation along with the lumped capacity points. In this worst case the manual, lumped capacity solution gave a q_{max} value that was only 16% high. An error analysis (*17*) gave 6.5% maximum probable error for the q_{max} data we present here. The maximum probable errors for q_{maxF} and R' were only 1.2 and 2.3%, respectively.

The present q_{max} data are presented in Table 1. The temperature difference observed at $q = q_{max}$ is also reported for the reader's interest. With these data we include six points which we reduced from temperature versus time plots made by Hendricks and Baumeister (*18*) in connection with a recent study of film boiling from small spheres (*19*) of both copper and tungsten carbide.

These results have been nondimensionalized in accordance with Equation (2), using property values as assembled by Reich and Lienhard (*20*). The resulting $q_{max}/$

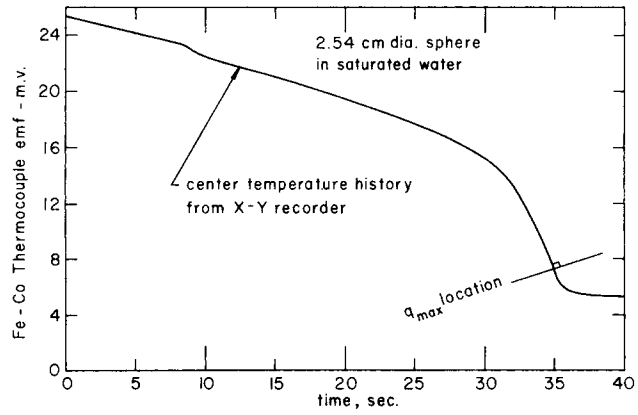

Fig. 5. Typical time versus center-temperature history for a quenched sphere.

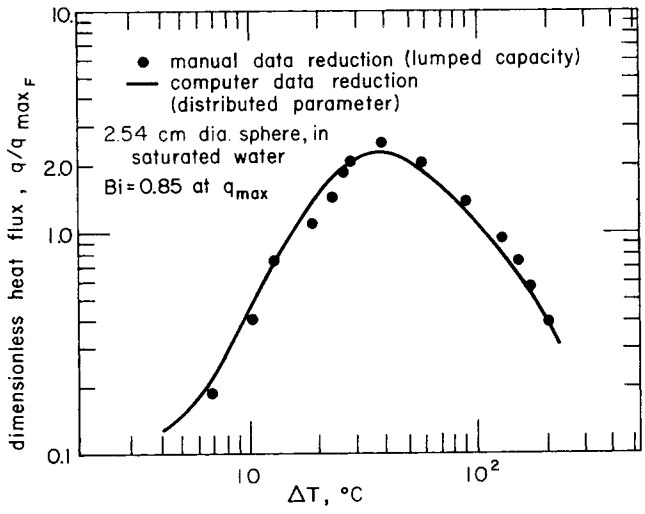

Fig. 6. Comparison of lumped capacity solution with distributed parameter solution.

TABLE 1. PEAK HEAT FLUX DATA FOR SPHERES

R, cm.	$q_{max}(10^5$ $J/m^2 \cdot S)$	ΔT_{max}, °C.	R'	$\frac{q_{max}}{q_{maxF}}$
Liquid nitrogen, $q_{maxF} = 156{,}000\ J/m^2 \cdot S$				
1.27*	1.18	8.1	12.01	0.75
1.27	1.25	7.0	↓	0.80
1.27*	1.39	8.9	↓	0.885
1.27	1.15	9.5	↓	0.73
1.27	1.06	10.5	↓	0.675
0.635*	0.95	11.1	6.0	0.606
0.635	1.14	11.7	↓	0.73
0.635*	1.12	9.4	↓	0.71
0.635	1.23	10.0	↓	0.784
0.635*	1.33	9.2	↓	0.848
0.635	1.38	10.6	↓	0.883
0.318*	1.43	11.7	3.0	0.91
0.318	1.79	10.5	↓	1.12
0.198[H]	1.80	8.9	1.87	1.14
0.198[H]	2.50	9.7	↓	1.59
0.0794*,[H]	2.43	7.0	0.75	1.55
0.0794[H]	3.04	9.2	↓	2.14
0.0397*,[H,T]	4.06	7.8	0.375	2.60
0.0198[H,T]	4.98	7.5	0.1875	3.19
Water, $q_{maxF} = 1{,}108{,}000\ J/m^2 \cdot S$				
1.27*	8.20	38.9	5.06	0.739
1.27	9.10	43.9	↓	0.82
1.27*	10.09	47.2	↓	0.91
1.27	8.76	40.5	↓	0.79
0.635	7.76	45.5	2.53	0.69
0.635*	8.93	41.6	↓	0.80
0.635	11.10	40.0	↓	1.01

* denotes runs for which motion pictures were made.
[H] denotes results from time-temperature data supplied by Hendricks (*19*).
[T] denotes tungsten-carbide sphere (all other spheres were copper).

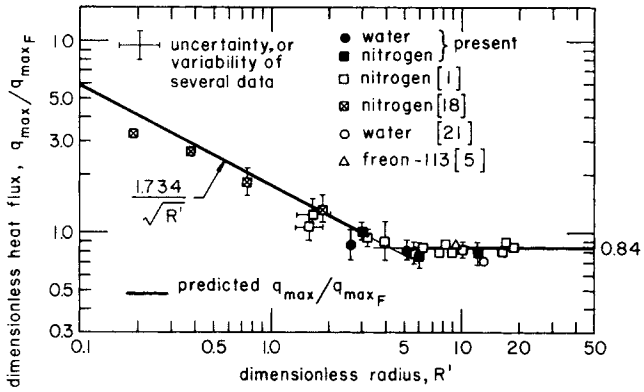

Fig. 7. Comparison of prediction with experimental data.

q_{max_F} values are plotted against R' in Figure 7 along with the q_{max} of Merte and Clark (*1*), Veres and Florschuetz (*5*), and Bradfield (*21*). On these coordinates the data correlate well—generally within the ± 15% scatter that is characteristic of q_{max} data. This serves to verify the assumptions underlying Equation (2) and to justify our expectation that $\Delta = \Delta(R')$.

VISUAL STUDY AND δ RESULTS

Figure 8 shows typical photographs of boiling from spheres of increasing R'. The first picture, Figure 8a, was taken from a motion picture supplied to us by Hendricks (*18*). The remaining three were obtained from our Hycam movies (1000 pictures/sec. at 1/5000 sec.). The quality of the reproductions has suffered somewhat because they had to be obtained from 16mm. reversal (positive) film. Nevertheless they show unmistakable evidence of the assumed analytical models.

In Figure 8a one-half of a Rayleigh wave is apparent in the escaping jet. This wavelength is comparable with $2\pi R$ as we anticipated. Figures 8c and 8d provide a side-view of the anticipated four-jet pattern for large R' although the jets are very blunt—much too short to contain a Rayleigh wave. Figure 8b is for a case close to the transitional range of R' and the single-jet configuration has deteriorated into an ambiguous conglomerate between the two models. These pictures are, of course, only static representations of processes that were repeatedly clear to the eye when the movies were screened.

Measurements of δ were made as indicated in Figure 1, using a motion picture screen. This was done by marking the boundary of the bubble-free sphere at the end of the movie, and then rerunning it in a stopaction projector to measure δ against this mark. Figure 9 presents these results in dimensionless form, for the available motion pictures—both ours and those made available to us by Hendricks (*18*).

These data are well represented by two straight lines—one for the small R' range and one for the large R' range:

$$\Delta_{\text{large } R'} \simeq 0.134\, R' \qquad (15)$$

and

$$\Delta_{\text{small } R'} \simeq 0.20\, R' \qquad (16)$$

The latter expression can be written as $\delta = 0.20\, R$ and substituted in Equation (6) to give $R_j = 0.94\, R$. Thus we might have avoided the need for δ data by adopting the assumption that $R_j = R$, and obtained essentially the same result (see footnote on page 339).

Equation (15) can be substituted in Equation (12), as we have noted already, to give

$$\left.\frac{q_{max}}{q_{max_F}}\right|_{\text{large } R'} = 0.84; \quad R' > \pi\sqrt{3} = 5.44 \qquad (17)$$

And the substitution of Equation (16) in Equation (11) gives

$$\left.\frac{q_{max}}{q_{max_F}}\right|_{\text{small } R'} = \frac{1.734}{\sqrt{R'}}; \quad R' < \pi \qquad (18)$$

Equations (17) and (18) have been included in Figure 7. These theoretical expressions lie within the intrinsic scatter of the data. The data within the transition region fall in such a way that it is permissible to use Equations (17) and (18) up to their point of intersection, defined by

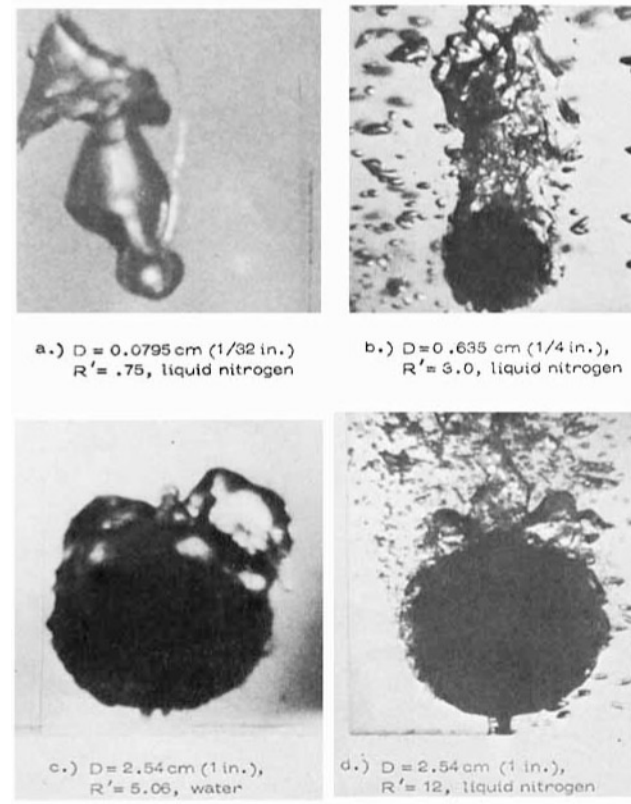

Fig. 8. Photographs of vapor jets near q_{max} on spheres of increasing diameters in liquid nitrogen and water.

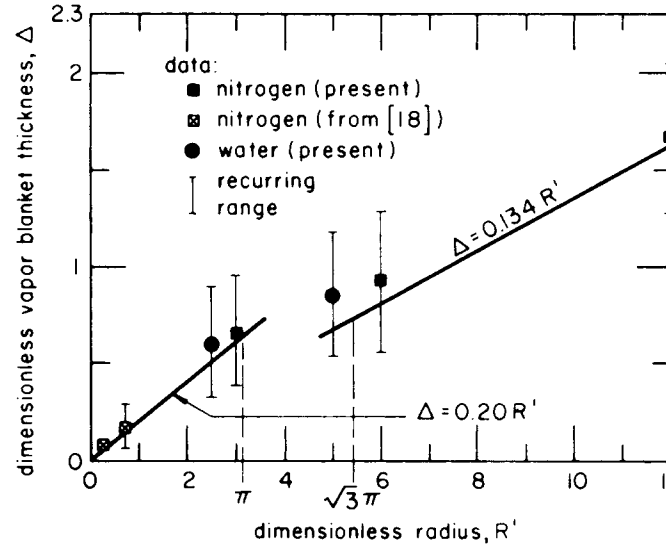

Fig. 9. Observed vapor blanket thickness.

$$\frac{1.734}{\sqrt{R'}} = 0.84 \quad \text{or} \quad R'_{\text{intersection}} = 4.26$$

Prior studies of boiling from cylinders (*10*, 22) suggest a limitation to Equation (18). When R' falls below 1/10 during boiling from cylinders, surface forces overbalance the diminishing force of gravity and the hydrodynamic mechanisms deteriorate to a point at which the peak heat flux ceases to exist in the boiling curve. Although we have no observations to prove that this is also the case for spheres, there is enough similarity between the processes to suggest a similar limitation in the present results. While few spheres are this small at earth normal gravity such a limitation is of great importance for reduced gravity applications. We must therefore avoid claiming validity of the present models for $R' \tilde{<} 1/10$.

CONCLUSION

The peak heat flux during saturated pool boiling from spherical heaters is given by

$$\frac{q_{\max}}{q_{\max F}} = \frac{1.734}{\sqrt{R'}}; \quad 0.1 \tilde{<} R' \bar{<} 4.26$$

and

$$\frac{q_{\max}}{q_{\max F}} = 0.84; \quad R' \geq 4.26$$

ACKNOWLEDGMENT

This work was supported in part under NASA Grant NGR/18-001-035, with T. H. Cochran as Project Manager.

NOTATION

A_j = area of jet, or combined area of all jets from a sphere
Bi = Biot number, hR/k
$c_p(T)$ = specific heat of heater material, a function of T
g = acceleration of gravity or other local body force field
h = heat transfer coefficient
h_{fg} = latent heat of vaporization
k = thermal conductivity of heater material
$q_{\max}$ = peak boiling heat flux
$q_{\max F}$ = $q_{\max}$ for an infinite horizontal flat plate as given by Equation (1)
R = radius of spherical heater
R' = dimensionless R given by Equation (2)
R_j = radius of a jet
T = temperature
t = time
U = critical vapor velocity at which jet becomes Helmholtz unstable
α = thermal diffusivity
δ = equatorial vapor blanket thickness
Δ = dimensionless vapor blanket thickness defined in the same way as R'
$\Delta T_{\max}$ = difference between heater temperature and saturated liquid temperature evaluated at $q_{\max}$
Δt, Δr = increments of time and sphere radius in numerical computation
λ_d = most rapidly collapsing Taylor-unstable wavelength
λ_H = Helmholtz unstable disturbance in vapor jet
ρ_f, ρ_g = saturated liquid and vapor densities, respectively
ρ_h = density of spherical heater material
σ = surface tension between saturated liquid and vapor

LITERATURE CITED

1. Merte, H. Jr., and J. A. Clark, "Boiling Heat Transfer with Cryogenic Fluids at Standard, Fractional and Near-Zero Gravity," *J. Heat Transfer, Trans. ASME, Ser. C*, **86**, 351 (1964).
2. Lewis, E. W., H. Merte Jr., and J. A. Clark, "Heat Transfer at 'Zero Gravity'," 55th Natl. Meeting, Am. Inst. Chem. Engrs., Houston (1965).
3. Zuber, N., "Hydrodynamic Aspects of Boiling Heat Transfer," AEC Report No. AECU-4439, Physics Math. (1959).
4. Bergles, A. E., and W. G. Thompson, Jr., "The Relationship of Quench Data to Steady-State Pool Boiling Data," *Intern. J. Heat Mass Transfer*, **13**, 55 (1970).
5. Veres, D. R., and L. W. Florschuetz, "A Comparison of Transient and Steady-State Pool-Boiling Data Obtained Using the Same Heating Surface," *J. Heat Transfer, Trans. ASME, Ser. C*, **93**, 229 (1971).
6. Bobrovich, G. I., I. I. Gogonin, and S. S. Kutateladse, "Influence of Size of Heater Surface on the Peak Pool Boiling Heat Flux," *J. Applied Mech. Tech. Phys.*, (ПМТФ), 4, 137 (1964).
7. Lienhard, J. H., and K. Watanabe, "On Correlating the Peak and Minimum Boiling Heat Fluxes with Pressure and Heater Configuration," *J. Heat Transfer, Trans. ASME, Ser. C*, **88**, 94 (1966).
8. Lienhard, J. H., "Interacting Effects of Gravity and Size upon the Peak and Minimum Pool Boiling Heat Fluxes," NASA CR-1551 (May, 1970).
9. Lienhard, J. H., and P.T.Y. Wong, "The Dominant Unstable Wavelength and Minimum Heat Flux on a Horizontal Cylinder," *J. Heat Transfer, Trans. ASME, Ser. C*, **86**, 220 (1964).
10. Sun, K. H., and J. H. Lienhard, "The Peak Pool Boiling Heat Flux on Horizontal Cylinders," *Intern. J. Heat Mass Transfer*, **13**, 1425 (1970).
11. Bellman, R., and R. H. Pennington, "Effects of Surface Tension and Viscosity on Taylor Instability," *Quart. App. Math.*, **12**, 151 (1954).
12. Zuber, N., M. Tribus, and J. W. Westwater, "The Hydrodynamic Crisis in Pool Boiling of Saturated and Subcooled Liquid," *Int. Develop. Heat Transfer, ASME*, 230 (1963).
13. Dhir, V., "Some Notes on the Development of the Hydrodynamic Theory of Boiling," Univ. Kentucky, T.R. No. 19-70-ME6 (March, 1970).
14. Lienhard, J. H., and V. Dhir, "Hydrodynamic Prediction of Peak Pool Boiling Heat Fluxes from Finite Bodies," submitted to *J. Heat Transfer*.
15. Lamb, Sir H., *Hydrodynamics*, 6th ed., Dover, New York (1945).
16. Berenson, P. J., "Transition Boiling Heat Transfer from a Horizontal Surface," M.I.T. Heat Transfer Lab. Tech. Rept. No. 17 (1960).
17. Ded, J. S., "The Peak Boiling Heat Flux on Spheres in Saturated Liquids," M.S. thesis, Univ. of Kentucky. Released as College of Engr. T.R. UKY-39-71-ME12 (July, 1971).
18. Hendricks, R. C., NASA Lewis Research Center, private communication (1971).
19. ———, and K. J. Baumeister, "Film Boiling from Submerged Spheres," NASA TN D-5124 (June, 1969).
20. Reich, R. A., and J H. Lienhard, "A Computer Program for Correlating Peak and Minimum Heat Fluxes," Univ. of Kentucky, Tech. Rept. UKY 34-71-ME9 (1971).
21. Bradfield, W. S., "On the Effect of Subcooling on Wall Superheat in Pool Boiling," *J. Heat Transfer, Trans. ASME, Ser. C*, **89**, 269 (1967).
22. Bakhru, N., and J. H. Lienhard, "On the Non-Existence of Peak and Minimum Boiling Heat Fluxes at Low Gravity," Univ. of Kentucky, College of Engineering, T.R. No. 18-70-ME5 (March, 1970).

Manuscript received July 21, 1971; revision received October 1, 1971; paper accepted October 5, 1971.